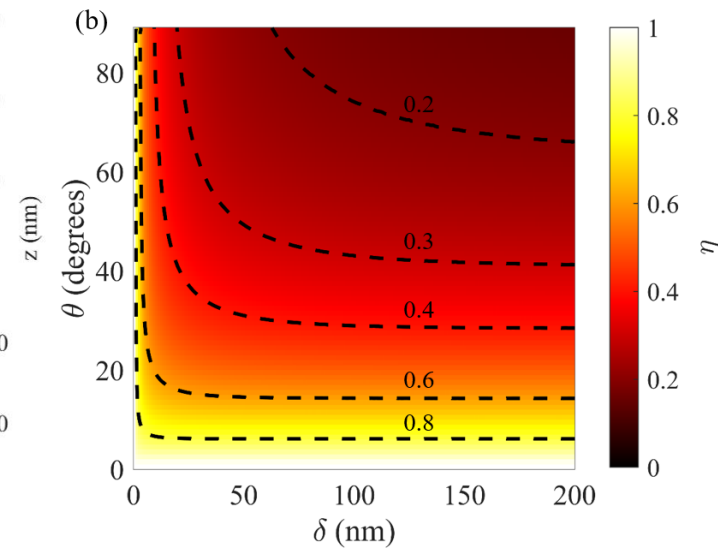
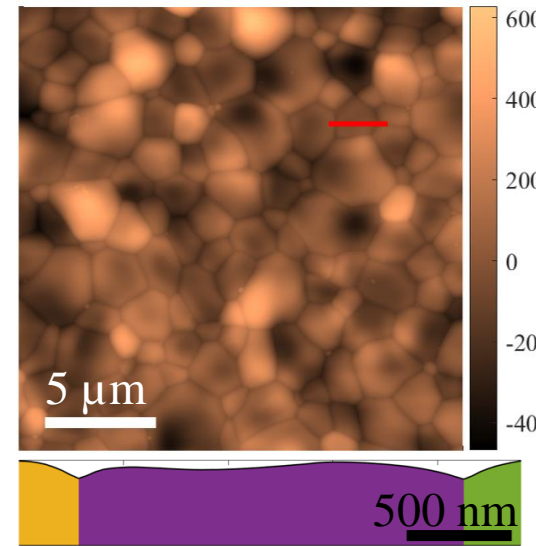


Analysis of Thermal Grooving Effects on Vortex Penetration in Vapor-Diffused Nb₃Sn

Based on our recent work:

<https://arxiv.org/abs/2409.01569>

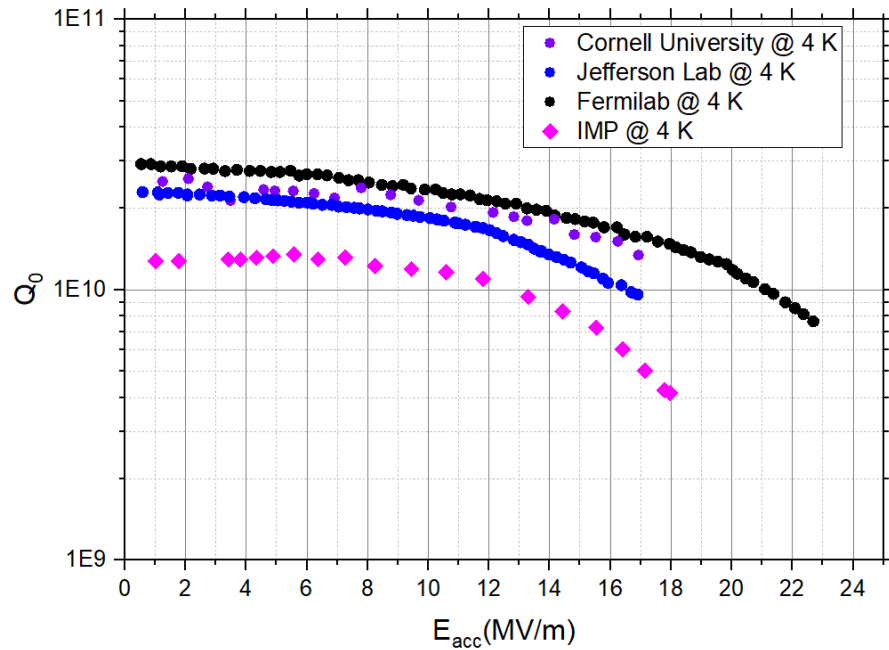


Eric M. Lechner

Jefferson Lab

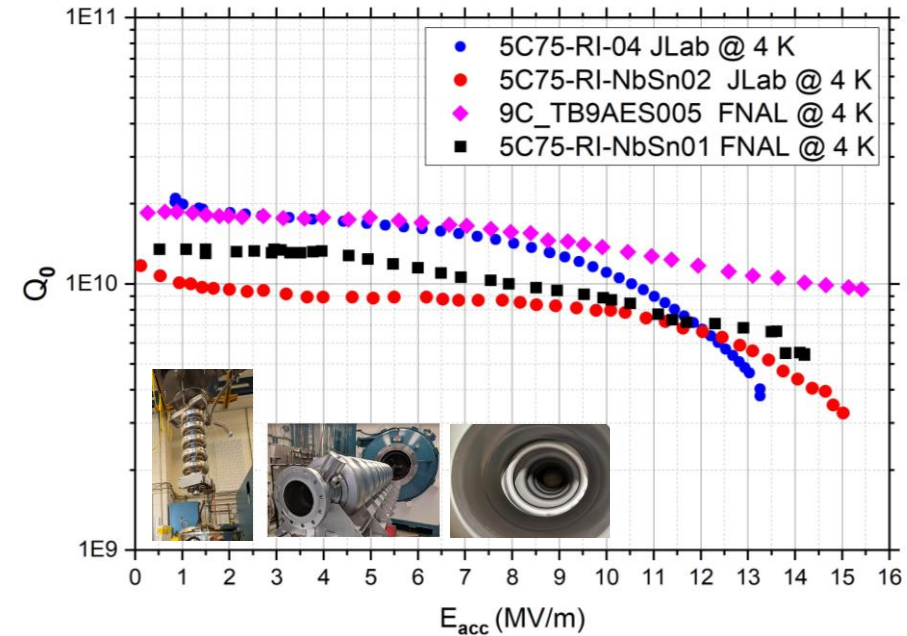
Performance of vapor-diffused Nb₃Sn grown on Nb

R&D 1.3/1.5 GHz single-cell cavity performance



- 1.3/1.5GHz single-cell cavities can attain an accelerating gradient over 20MV/m with $Q \sim 10^{10}$.
- Cavities of various frequencies (650MHz, 952MHz, 2.6GHz, 3.6GHz) coated at different facilities show comparable performance.

Multi-cell cavity performance

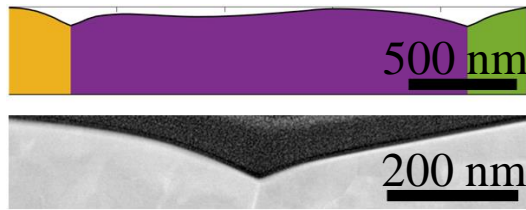
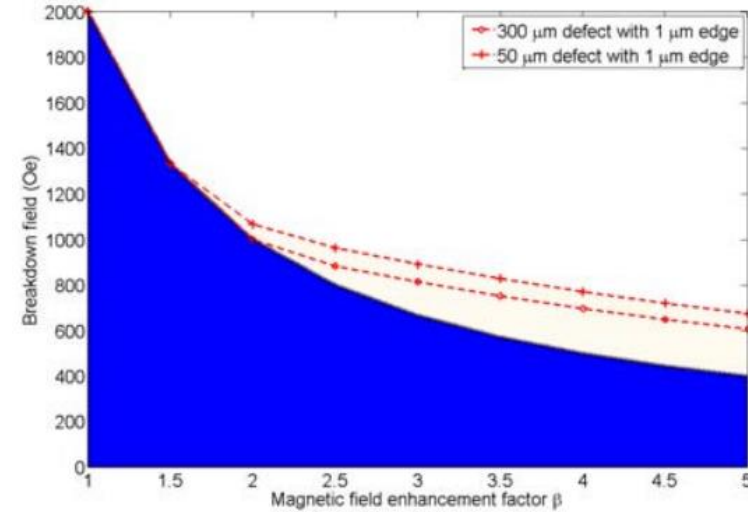
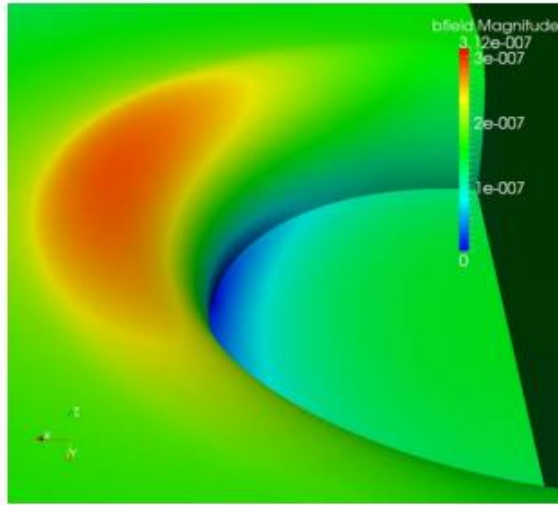
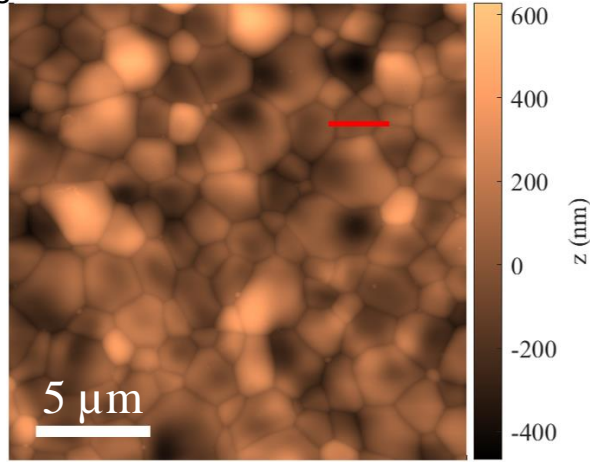


- 1.5GHz five-cell and 1.3GHz 9-cell cavities were demonstrated to reach $Q \sim 10^{10}$ at 10MV/m at 4.4K.
- Maximum gradients achieved up to ~ 20 MV/m.

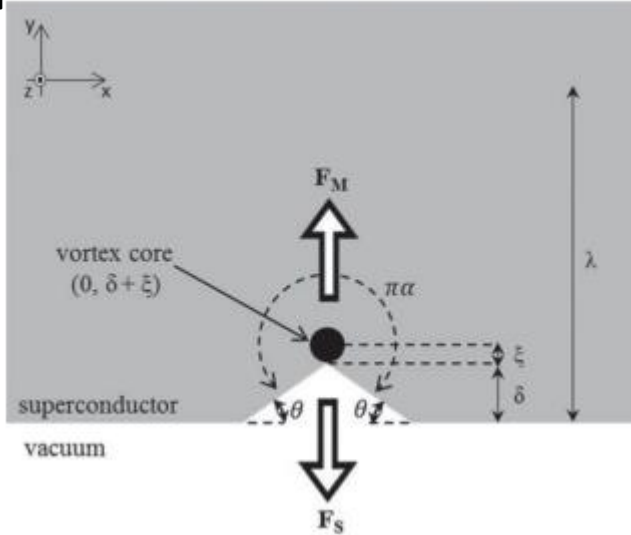
U.Pudasaini et al. "Managing Sn-Supply to Tune Surface Characteristics of Vapor-Diffusion Coating of Nb₃Sn", presented at the SRF21, East Lansing, MI, USA, Jun.-Jul. 2021, doi:10.18429/JACoW-SRF2021-TUPTEV013.
 S. Posen et al. "Advances in Nb₃Sn superconducting radiofrequency cavities towards first practical accelerator applications" Superconductor Science and Technology. 2021 Jan 11;34(2):025007.
 D. Hall, "New Insights into the Limitations on the Efficiency and Achievable Gradients in Nb₃Sn SRF Cavities", PhD thesis, Cornell University (2017).
 G. Jiang et al.. Understanding and optimization of the coating process of the radio-frequency Nb₃Sn thin film superconducting cavities using tin vapor diffusion method. Applied Surface Science. 2024 Jan 15;643:158708.
 G. Ereemeev "Progress in Nb₃Sn developments for CEBAF-style quarter cryomodule" TTC-2022,

Introduction – Topographic Defects

Nb₃Sn is topographically imperfect [3]

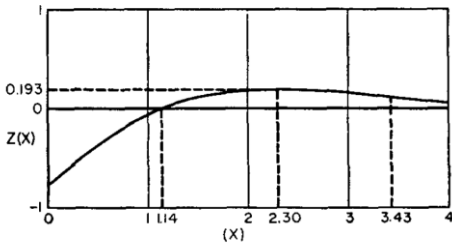


[4]



- Topographic defects produce local field enhancements due to the nature of the Meissner current. It has been proposed that this may turn regions of the cavity normal conducting and lead to thermal instabilities.
- Topographic defects may also reduce the local superheating fields. This reduces the field required to nucleate dissipative vortex semiloops and trigger thermal instabilities.

[1]



[2]

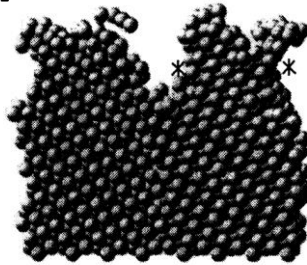


FIG. 3. Normalized profile shape due to surface diffusior

Step 210,000

[3] Xie , et al. Quench Simulation Using a Ring-Type Defect Model SRF'11, 2011

[4] Kubo, Takayuki, *Progress of Theoretical and Experimental Physics* 2015.6 (2015): 063G01.

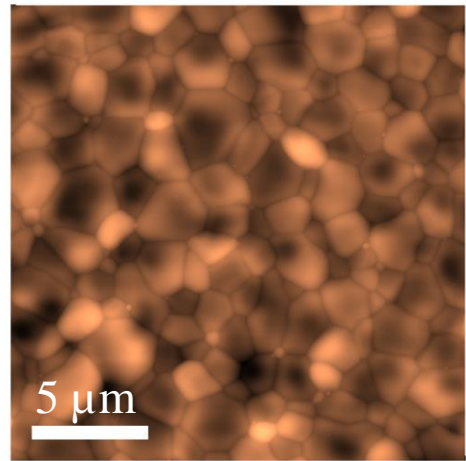
[1] Mullins, W.W., 1957. *Journal of Applied Physics*, 28(3), pp.333-339.
 [2] Iwasaki, Tomio, et al. *JSME international journal. Ser. A, Mechanics and material engineering* 40.1 (1997): 15-22.

Topography Nb₃Sn – Evolution with Coating Duration

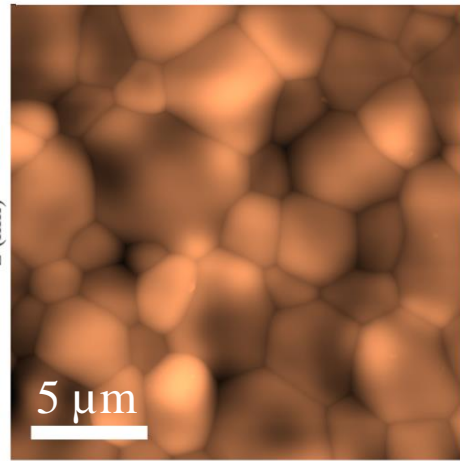
Investigation

- Study samples coated from 1 to 78 hours (6 samples)
- 10x areas randomly sampled via AFM from each sample

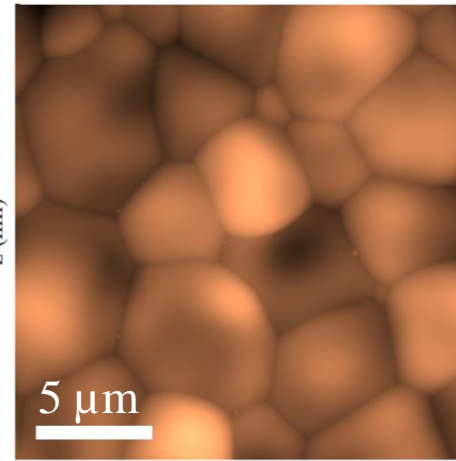
Coating Duration – 1 hr



Coating Duration – 6 hr



Coating Duration – 18 hr



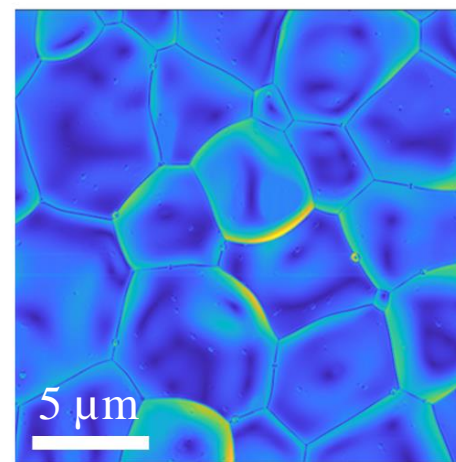
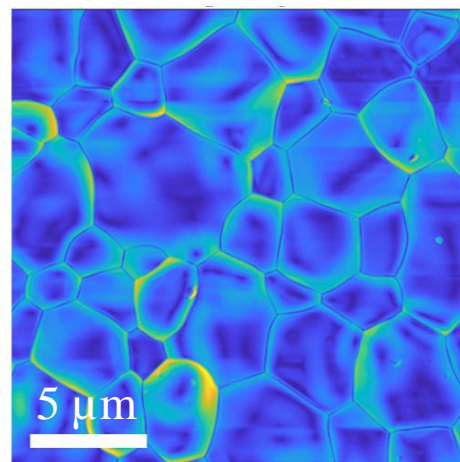
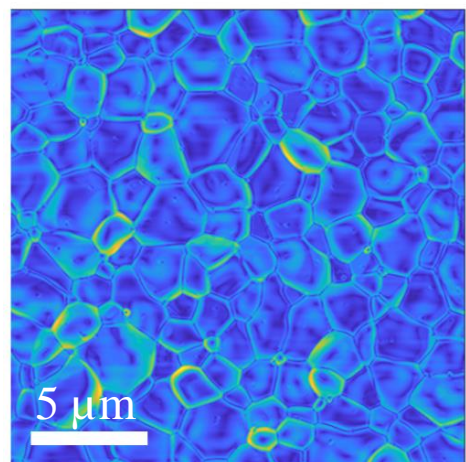
Increased coating duration results in:

- Thickening of the coating
- Grain growth
- Roughening of the surface
- Grooves are on the order of 100 nm deep (comparable to the penetration depth)

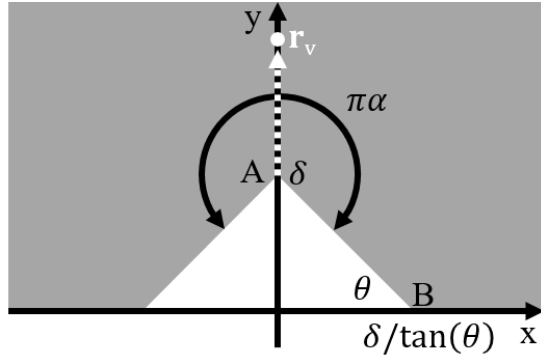
Slope angle calculation

$$\cos \theta = \hat{\mathbf{z}} \cdot \hat{\mathbf{n}} = \hat{\mathbf{z}} \cdot \frac{(-h_x, -h_y, 1)}{(1 + h_x^2 + h_y^2)^{1/2}}$$

- Access to h_x, h_y is given by the extension of the Savitzky-Golay filter for surfaces [1]
- High slope angles exist regardless of coating duration



Superheating Field Suppression



Limitations:

Calculation is performed in the London theory

1. Neglects the BCS current-field relation

Force on vortex from magnetic field

$$\mathbf{F}_M = \mathbf{J}_M \times \phi_0 \hat{\mathbf{z}}$$

$$\nabla^2 B_z = \frac{1}{\lambda^2} B_z$$

$$\mathbf{J}_M = \nabla \times \mathbf{B} / \mu_0$$

$$\epsilon(\mathbf{r}) = |\mathbf{J}(\mathbf{r})| / J_0$$

Force from the surface: $\mathbf{J}_{V+I} \cdot \hat{\mathbf{n}} = 0$

$$\mathbf{F}_S = \mathbf{J}_I \times \phi_0 \hat{\mathbf{z}}$$

$$\frac{2\pi\mu_0\lambda^2}{\phi_0} \Phi_I(x, y) = \tilde{\Phi}_I(x, y) = \text{Re}(-i \ln(w - w_0^*))|_{w=F^{-1}(x, y)}$$

$$\mathbf{J}_I = -\nabla \Phi_I$$

$\mathbf{r}_v = (\delta + \xi) \hat{\mathbf{y}}$ - London theory vortex nucleation position

$\mathbf{F}_S + \mathbf{F}_M = \mathbf{0}$ - Condition for vortex nucleation

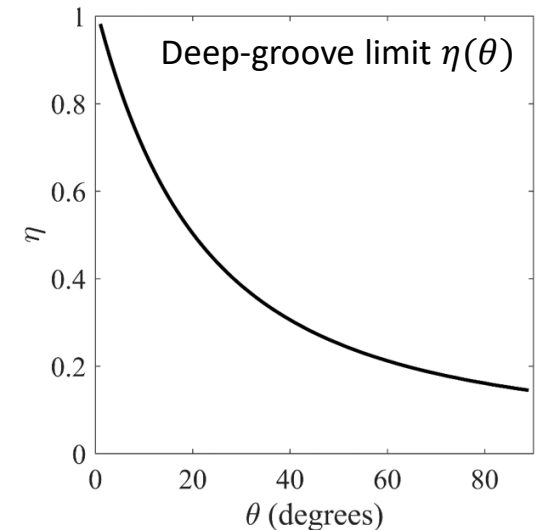
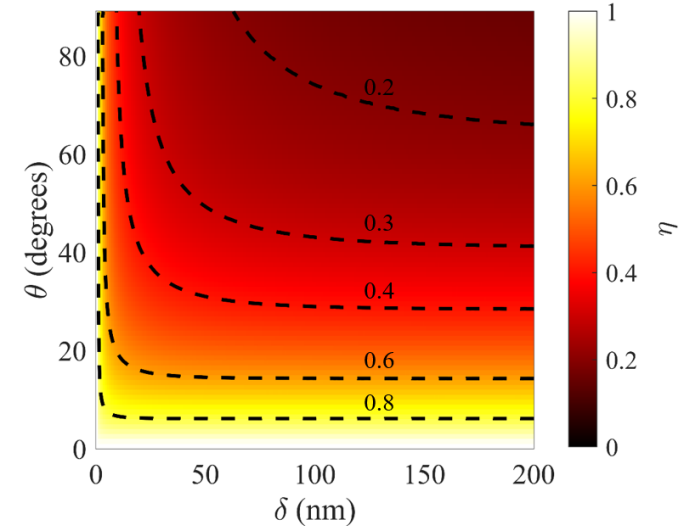
Geometrically suppressed B_s

$$B_s^* = \frac{2\xi |-\nabla \tilde{\Phi}_I(\mathbf{r}_v)|}{\epsilon(\mathbf{r}_v)} B_s$$

Superheating field suppression (SFS) factor

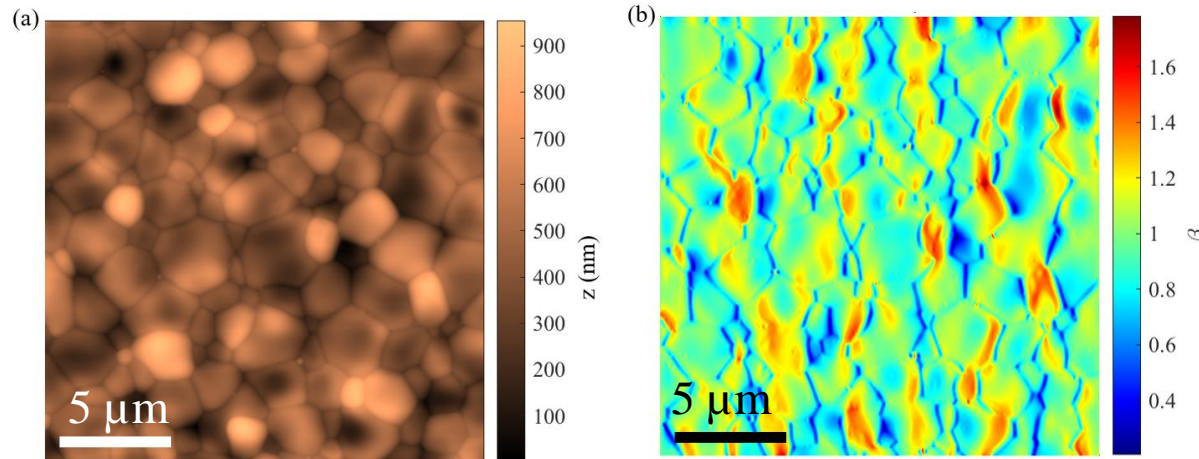
$$\eta(\xi, \lambda, \delta, \theta) = \frac{2\xi |-\nabla \tilde{\Phi}_I(\mathbf{r}_v)|}{\epsilon(\mathbf{r}_v)}$$

$\xi = 3 \text{ nm}$ and $\lambda = 120 \text{ nm}$
used to represent Nb_3Sn



MFE & SFS

Magnetic Field Enhancement Factor



[1] *Perfect Electrical Conductor Model*

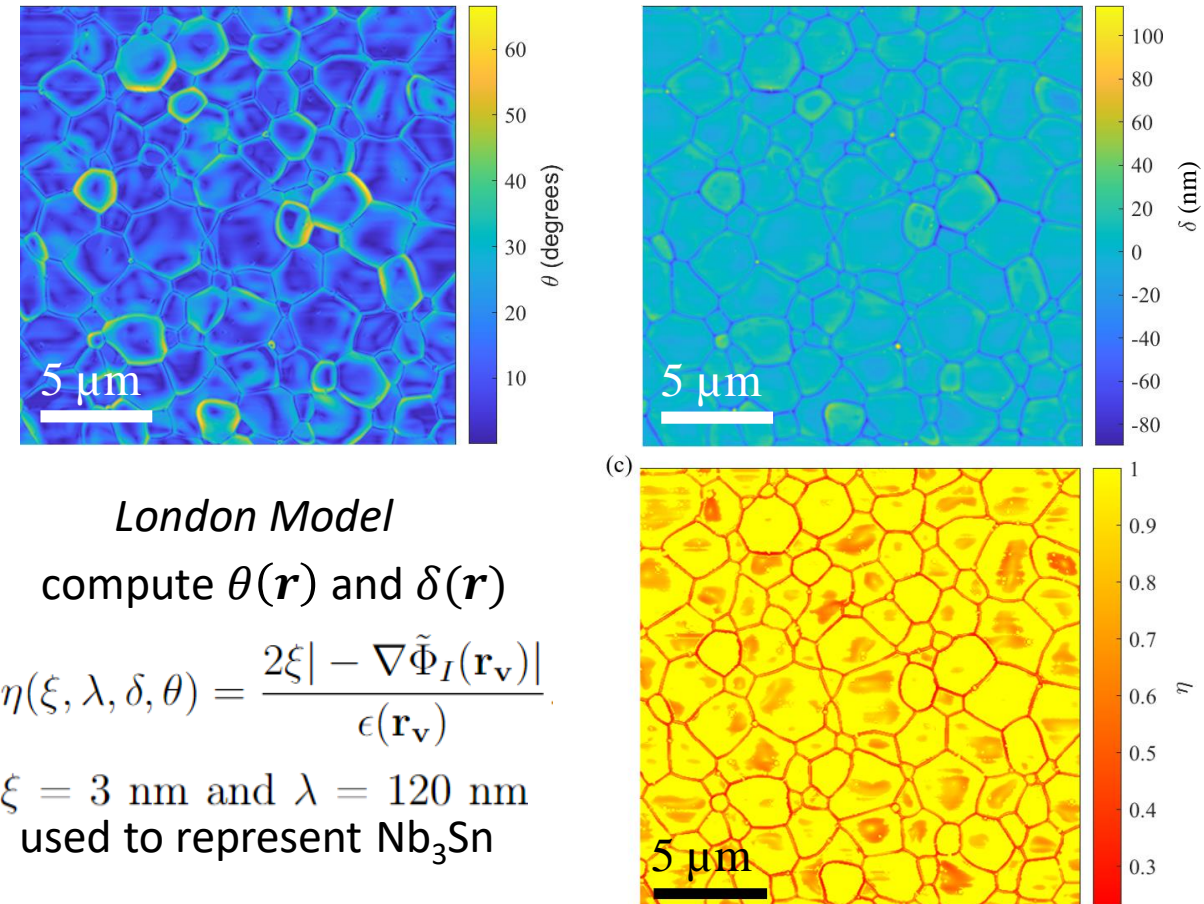
$$\beta(\mathbf{r}) = |\mathbf{B}(\mathbf{r})|/B_0$$

$$\nabla^2\psi = 0$$

$$\nabla\psi \cdot \hat{x} = B_0, \nabla\psi \cdot \hat{y} = 0 \text{ and } \nabla\psi \cdot \hat{n} = 0$$

$$\psi(x, y, z_{max} = 6 \mu m) = -B_0 x \quad \mathbf{B}(\mathbf{r}) = B_0 \hat{x}$$

Superheating Field Suppression Factor



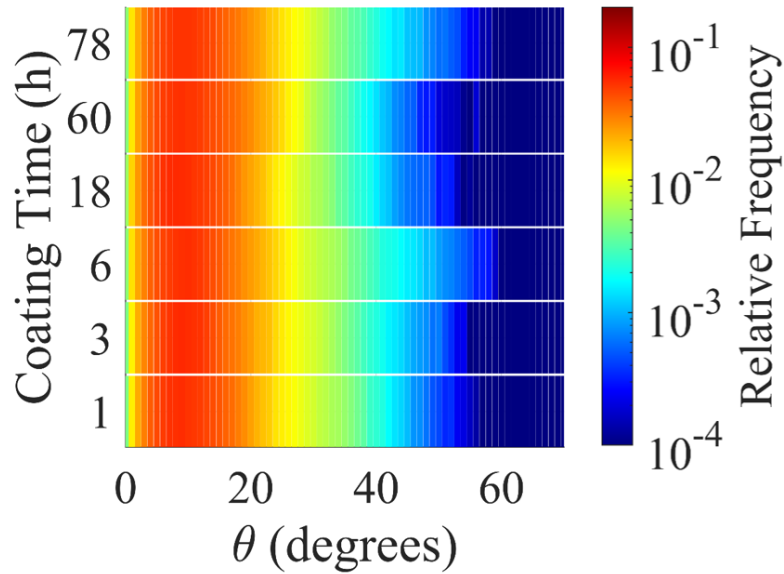
London Model

compute $\theta(\mathbf{r})$ and $\delta(\mathbf{r})$

$$\eta(\xi, \lambda, \delta, \theta) = \frac{2\xi |-\nabla\tilde{\Phi}_I(\mathbf{r}_v)|}{\epsilon(\mathbf{r}_v)}$$

$\xi = 3 \text{ nm}$ and $\lambda = 120 \text{ nm}$
used to represent Nb_3Sn

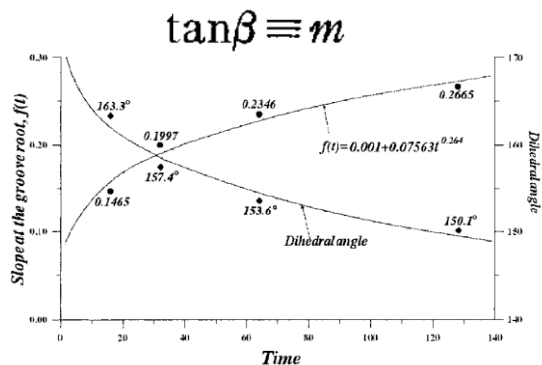
Results



- No obvious trend with slope angles

[1] Thermal grooves are often considered to retain the groove angle during annealing

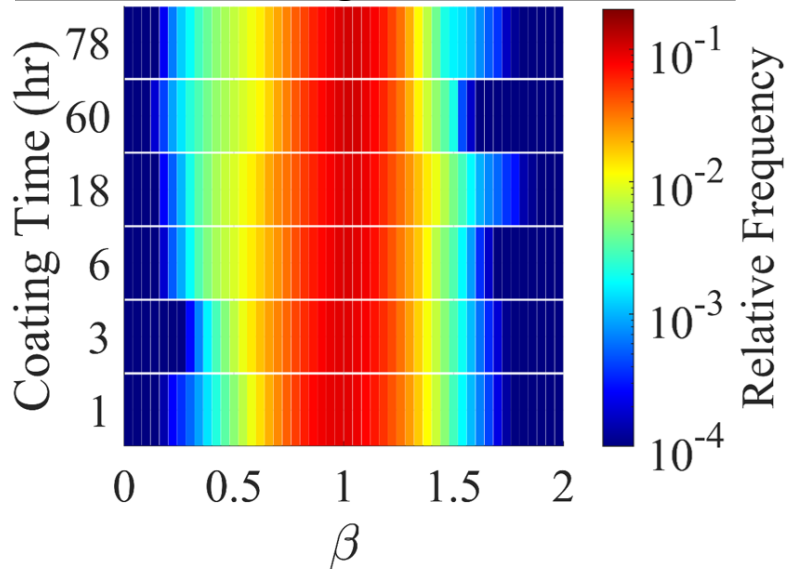
[2]



[1] Mullins, W.W., 1957. *Journal of Applied Physics*, 28(3), pp.333-339.

[2] Zhang, W., P. Sachenko, and J. H. Schneibel. *Journal of materials research* 17.6 (2002): 1495-1501.

Increased coating duration results in:



- No obvious trend with magnetic field enhancement factors.
- Peak MFE factors between 1.5 and 2

[1]

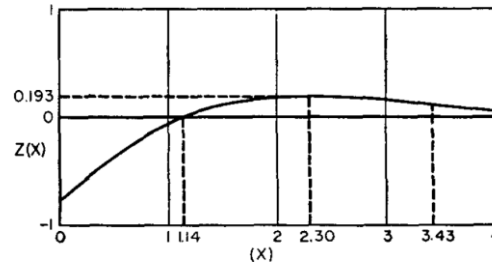
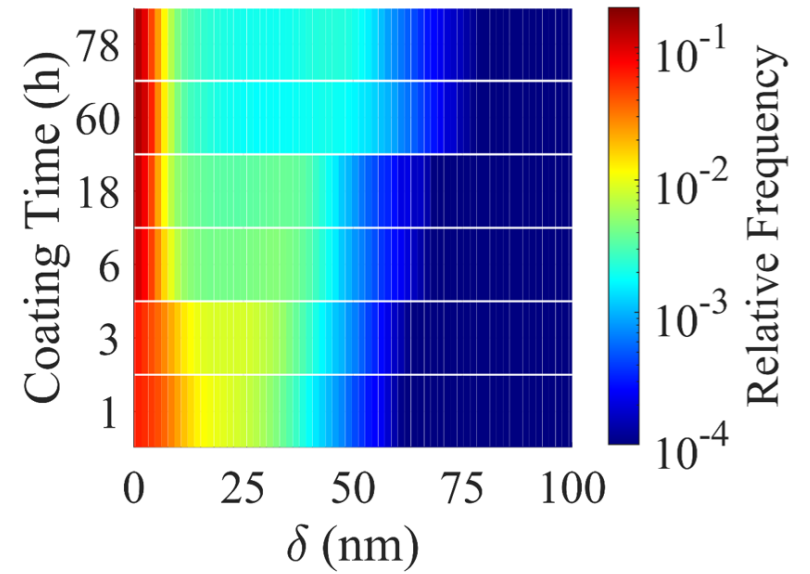


FIG. 3. Normalized profile shape due to surface diffusion.

$$y(x,t) = m(Bt)^{\frac{1}{2}} Z\left[\frac{x}{(Bt)^{\frac{1}{2}}}\right] - \text{self-similarity}$$

$$s = 4.6(Bt)^{\frac{1}{2}}$$

$$d = 0.973m(Bt)^{\frac{1}{2}}$$

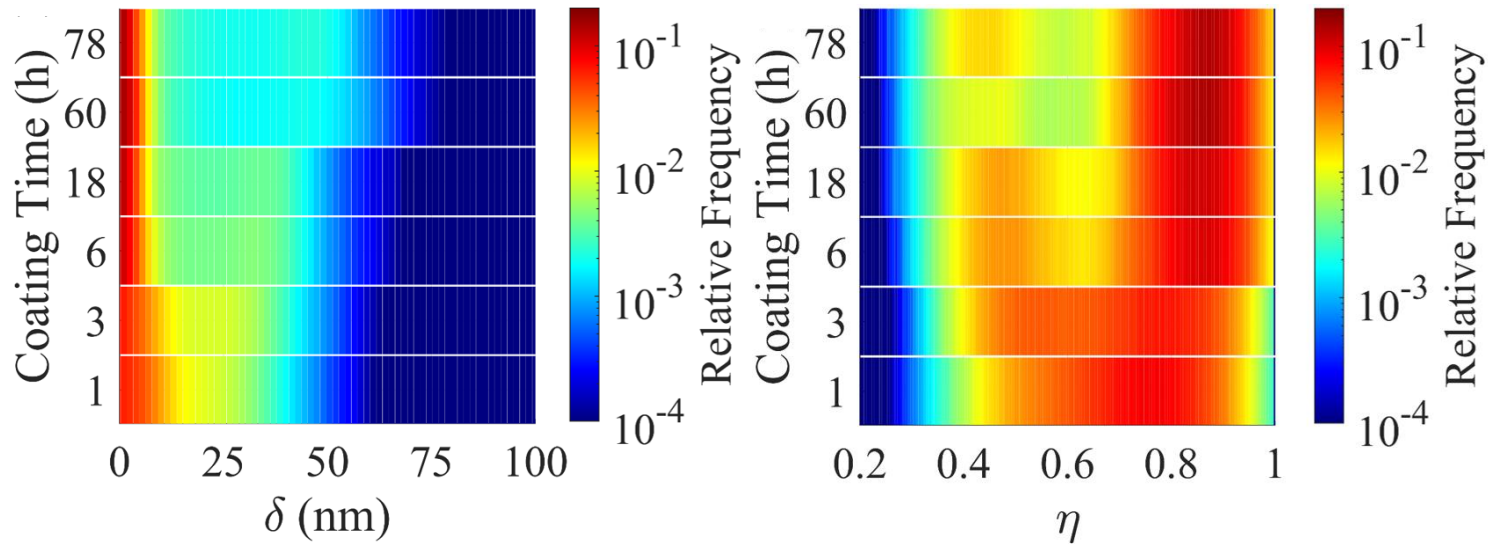


- Increase in groove depth is clearly observed

[1]

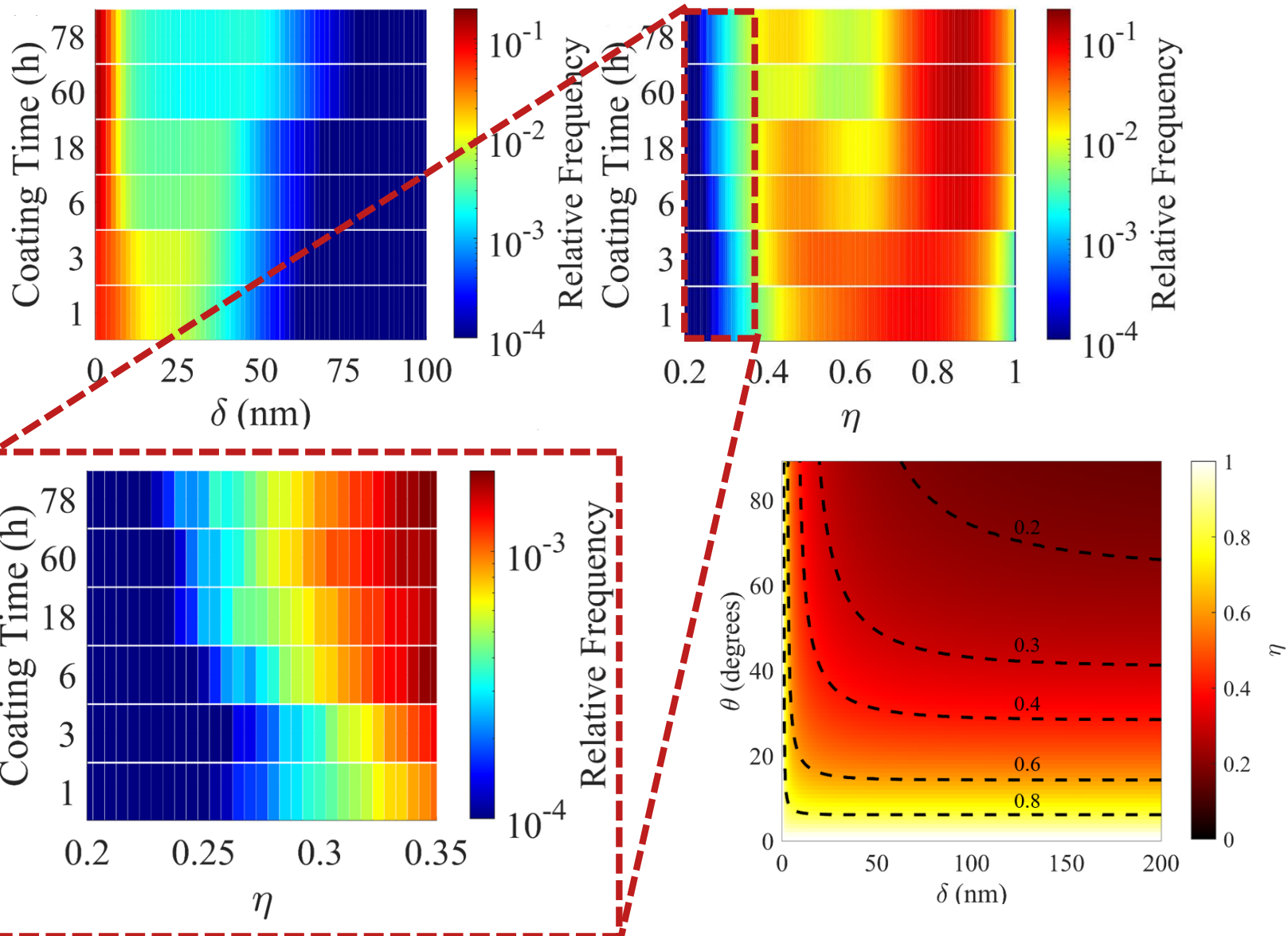
$$d = 0.973m(Bt)^{\frac{1}{2}}$$

Results



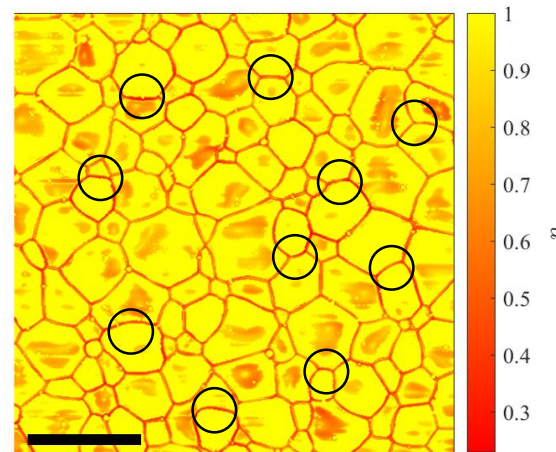
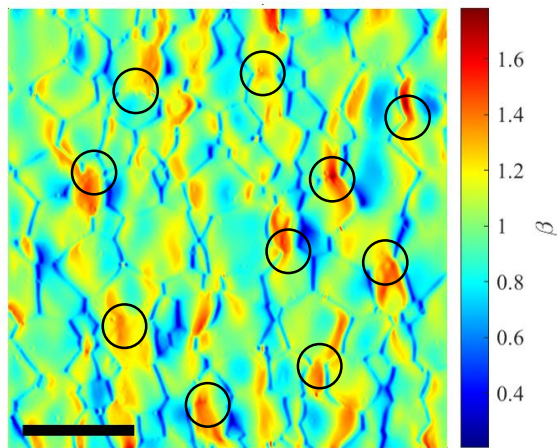
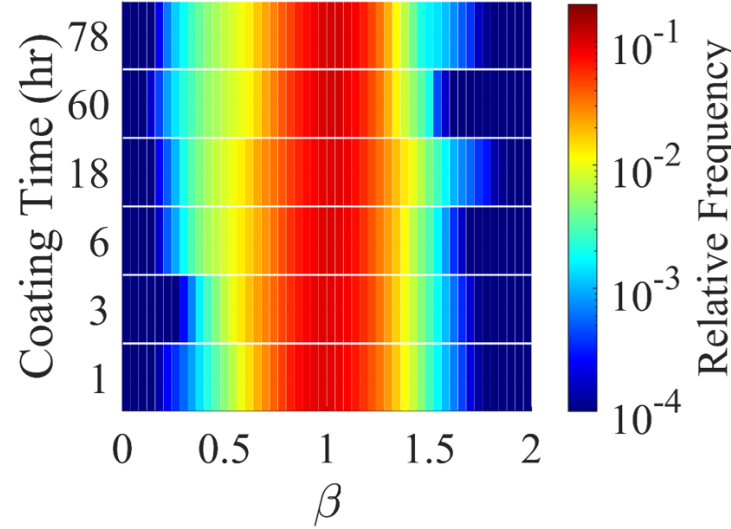
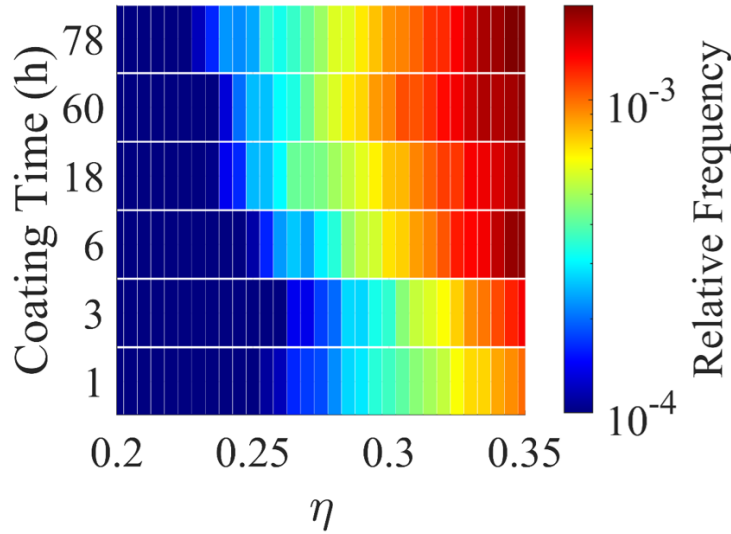
- Bifurcation in the deviation between background plane and the topography
- This bifurcation is more clearly reflected in the SFS factor. During short annealing times
- This bifurcation is more clearly reflected in the SFS factor. During short annealing times the distribution presented a merged bimodal distribution which bifurcates as coating time proceeds.

Results



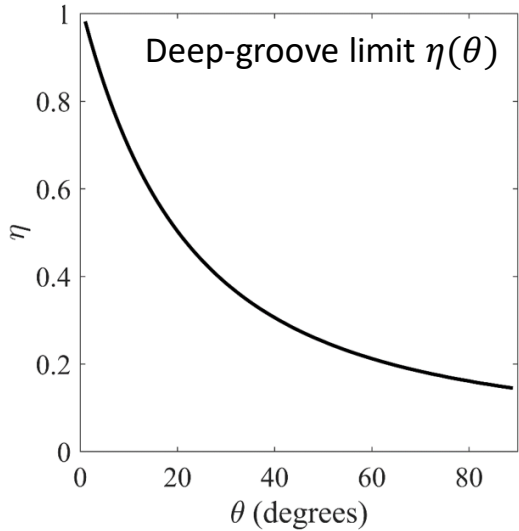
- Bifurcation in the deviation between background plane and the topography
- This bifurcation is more clearly reflected in the SFS factor. During short annealing times
- This bifurcation is more clearly reflected in the SFS factor. During short annealing times the distribution presented a merged bimodal distribution which bifurcates as coating time proceeds.

Discussion

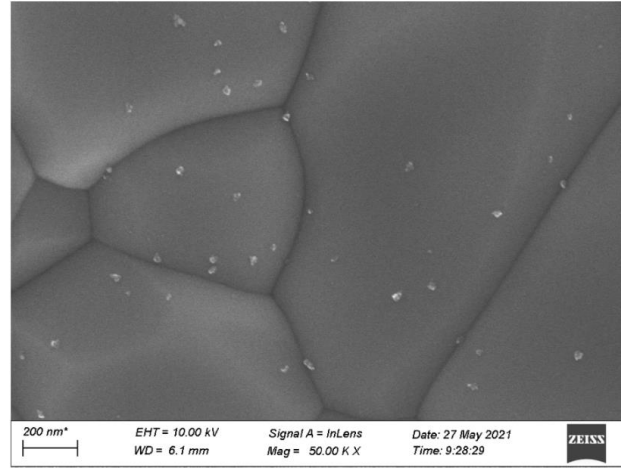


- Considering only the effects of superheating field suppression on the superheating field (~ 400 mT) peak magnetic fields of 107-128 mT may be expected.
- Peak magnetic field enhancement values fall around ~ 1.7 .
- There are many locations where MFE and SFS overlap. This may further reduce the field of vortex penetration by $B_{max}^* = \left(\frac{\eta}{\beta}\right) B_{max}$. The combined effect can reduce peak magnetic field to ~ 51 -77mT (12-18MV/m in TESLA-shaped cavities).
- While this is in qualitative agreement with the field limitation in Nb_3Sn , there are many loss mechanisms which should be considered *before* topography.

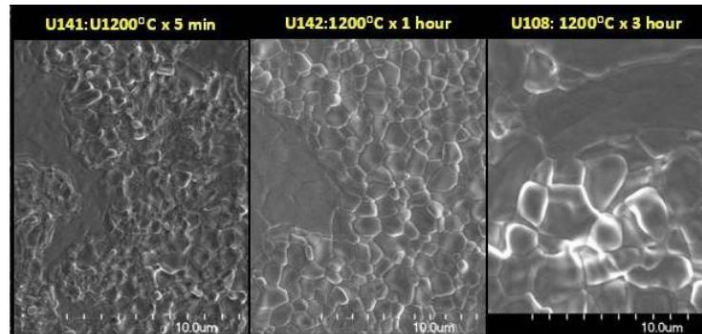
Discussion – Other Performance Limiting Mechanisms



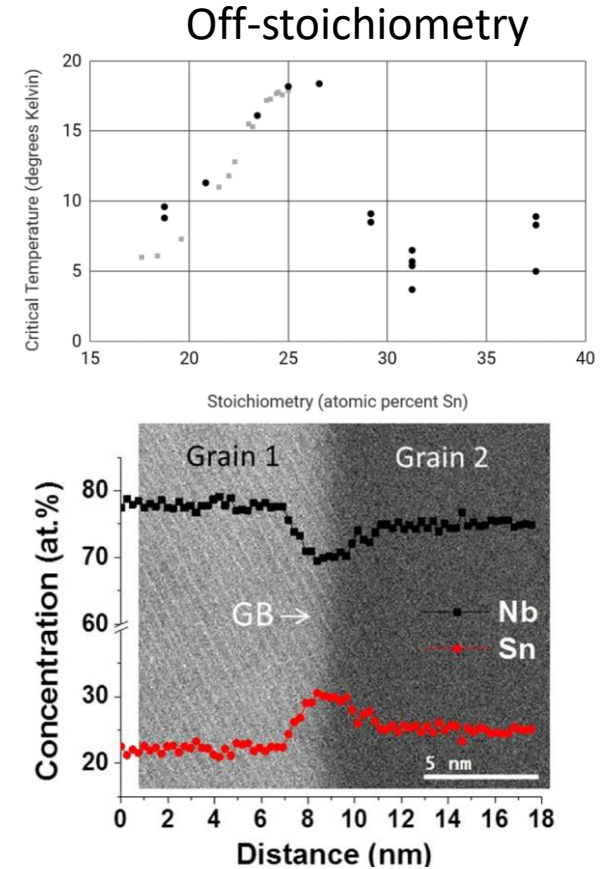
[1] Sn droplets



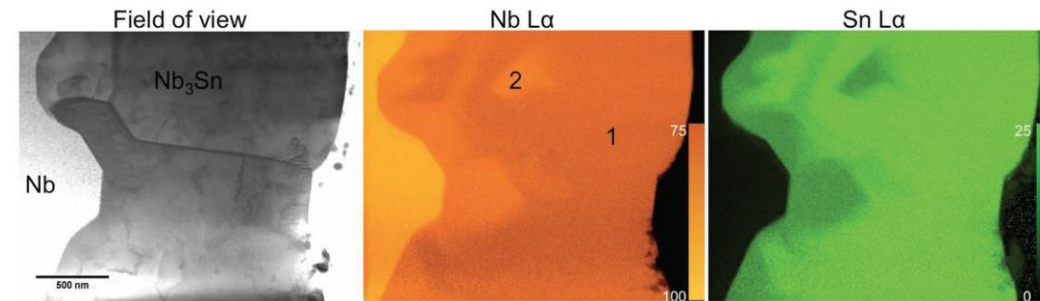
[2] Thin patchy regions



[3]



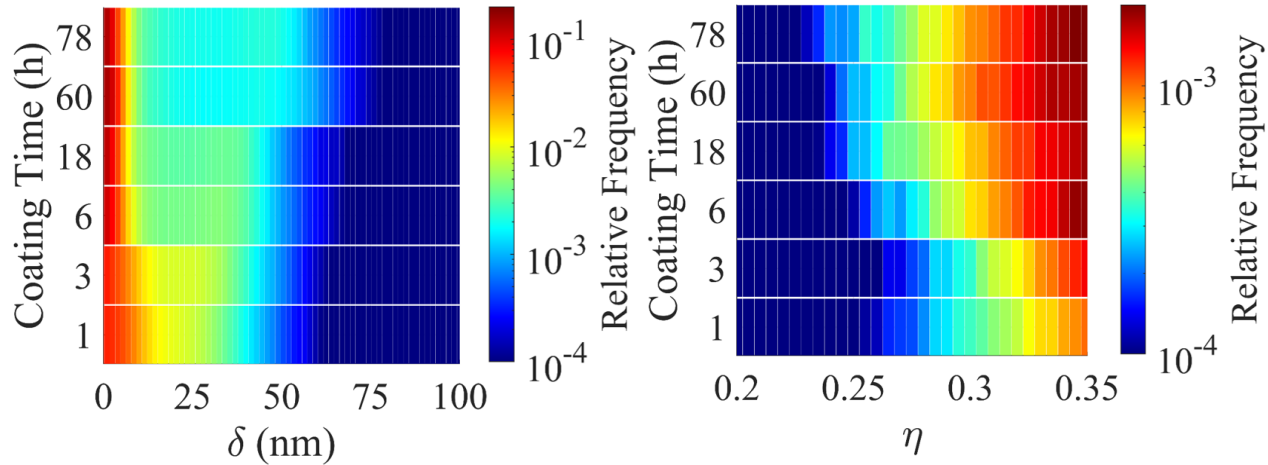
[4]



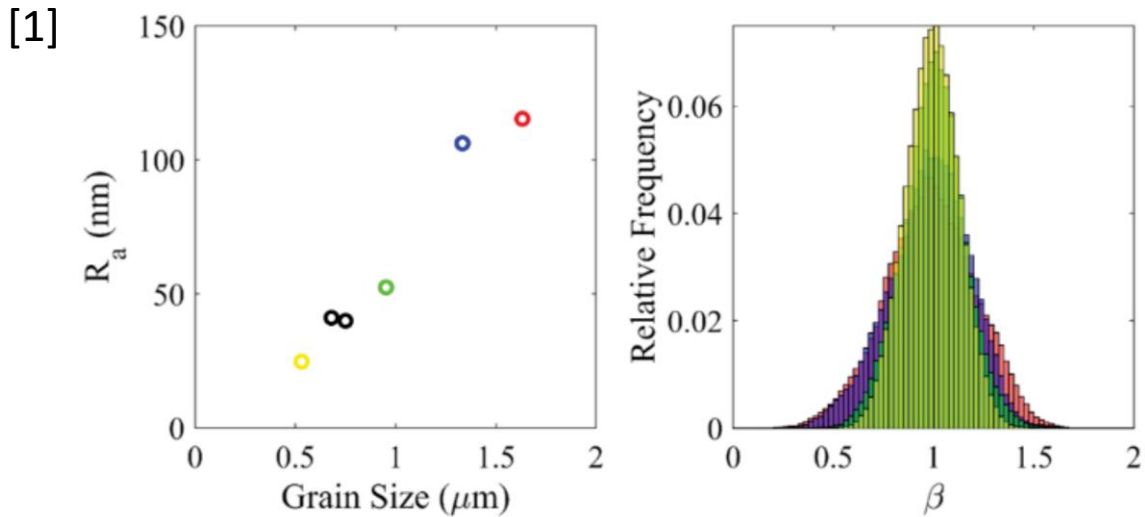
The deep-groove limit suggests that you should not see Q-slopes below 50 mT, yet many examples of this exist.

- [1] Jiang, Guangze, et al. *Applied Surface Science* 643 (2024): 158708
- [2] Pudasaini, Uttar, et al. *Proc. 18th Int. Conf. RF Superconductivity (SRF'17)*. 2017.
- [3] Carlson, Jared, et al. *Physical Review B* 103.2 (2021): 024516.
- [4] Becker, Chaoyue, et al. *Applied Physics Letters* 106.8 (2015).

Discussion – How Can The Suppression Factor Be Improved?



Short coating durations at 1200 °C tend to reduce groove depths



Temperature may play a role in surface

[2]

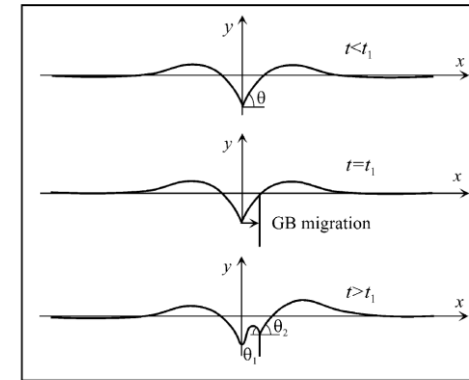


Fig. 9 A model of GB grooving with the instantaneous GB jump during annealing

Encourage grain boundary migration

[3]

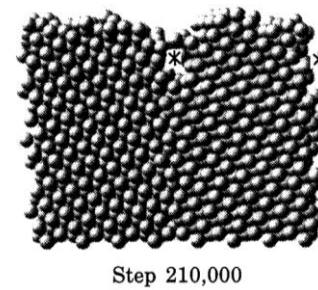
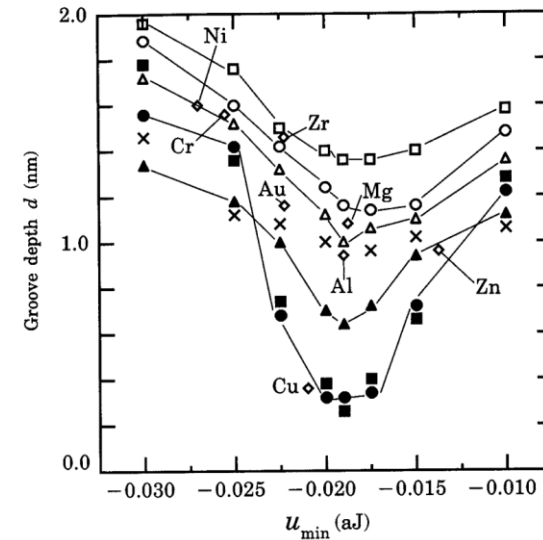


Fig. 8 Grain boundary grooving with Cu atoms at $T = 600 \text{ K}$

Include impurities



[1] U. Pudasaini et al. SRF'23 (Grand Rapids, MI, USA). JACoW Publishing, Geneva, Switzerland, 2023.

[2] Rabkin, E., et al. *Journal of materials science* 41 (2006): 5151-5160.

[3] Iwasaki, Tomio, et al. *JSME international journal. Ser. A, Mechanics and material engineering* 40.1 (1997): 15-22.

Conclusions & Future Work

Conclusions

- Developed a simple model to calculate the superheating field suppression factor in the London theory.
- We have shown that superheating field suppression may be a large contributor to peak field degradation in dense, stoichiometric Nb₃Sn. The effect of which is compounded by local magnetic field enhancement.
- We hope that this work inspires more physically justified theories to make estimates of the geometrically suppressed superheating field in the deeper type-II limit where Nb₃Sn resides.

Future work

- Compare the topography from witness samples and performance of Nb₃Sn coated cavities.

Acknowledgments

Coauthors

U. Pudasaini

O. Trofimova

J.W. Angle (PNNL)

M.C. DiGuilio (VT)

Others

G. Eremeev

M.J. Kelley

C.E. Reece